

Thermochemical Analysis of Phases Formed at the Interface of a Mg alloy-Ni-plated Steel Joint during Laser Brazing

ALI M. NASIRI, PATRICE CHARTRAND, DAVID C. WECKMAN,
and NORMAN Y. ZHOU

The thermodynamic stability of precipitated phases at the steel-Ni-Mg alloy interface during laser brazing of Ni-plated steel to AZ31B magnesium sheet using AZ92 magnesium alloy filler wire has been evaluated using FactSage thermochemical software. Assuming local chemical equilibrium at the interface, the chemical activity–temperature–composition relationships of intermetallic compounds that might form in the steel-Ni interlayer-AZ92 magnesium alloy system in the temperature range of 873 K to 1373 K (600 °C to 1100 °C) were estimated using the Equilib module of FactSage. The results provided better understanding of the phases that might form at the interface of the dissimilar metal joints during the laser brazing process. The addition of a Ni interlayer between the steel and the Mg brazing alloy was predicted to result in the formation of the AlNi, Mg₂Ni, and Al₃Ni₂ intermetallic compounds at the interface, depending on the local maximum temperature. This was confirmed experimentally by laser brazing of Ni electro-plated steel to AZ31B-H24 magnesium alloy using AZ92 magnesium alloy filler wire. As predicted, the formation of just AlNi and Mg₂Ni from a monotectic and eutectic reaction, respectively, was observed near the interface.

DOI: 10.1007/s11661-012-1520-y

© The Minerals, Metals & Materials Society and ASM International 2012

I. INTRODUCTION

MAGNESIUM and its alloys are currently under intense investigation for use in many applications in the automotive industry.^[1,2] As steel sheet is still the most commonly used material for fabrication of auto body structures, the ability to make hybrid structures of magnesium alloy and steel sheet would be desirable for many applications. This would allow the overall weight of the autobody to be reduced, resulting in better fuel efficiency and lower environmental impact. Therefore, there is increasing interest in identifying and developing new techniques and processes that can be used to make dissimilar joints between magnesium alloys and steel sheet.^[2–7]

It is well known that it is difficult to join magnesium alloys to steel by conventional fusion welding technologies.^[2] This can be attributed to the large difference in their melting temperatures and the nearly zero solubility of magnesium and iron.^[2] The melting point of steel [\approx 1823 K (1550 °C)] is well above the boiling point of magnesium [1380 K (1107 °C)], and this can cause catastrophic vaporization of the molten magnesium during a fusion welding process. In addition, the

maximum solid solubility of Fe in Mg is only 0.00041 at. pct Fe.^[2] There is also clear evidence that magnesium and steel do not react with each other and do not mix in the liquid state at ambient pressure.^[2] Thus, metallurgical bonding between these two metals will only be possible provided another element that can interact and bond with both of them can be applied between the Mg and Fe and act as an intermediate interlayer element.

The feasibility and benefits of using Cu, Sn, and Ni interlayers to join Mg and steel by various fusion welding processes have been investigated experimentally with varying degrees of success.^[5–7] More recently, Nasiri *et al.*^[8,9] have studied the use of Al and Ni interlayers when laser brazing these dissimilar metals using a Mg-Al alloy filler wire. However, identifying and evaluating an appropriate interlayer between steel and Mg alloys experimentally can be costly and time consuming. This process can be shortened with the use of computational thermodynamics, which provides a convenient way for predicting the phases most likely to form in complex multi-element alloy systems at the interface as a function of alloy composition and temperature with greater accuracy than is possible using the binary or ternary phase diagrams of the constituent elements. Prior knowledge of these phases can be beneficial as they can affect the mechanical properties, the temperature of the joint interface, the wettability of the steel by the magnesium alloy, and the overall brazeability of the joint.

In the last decade, several different commercial thermochemical codes have become available for the calculation of the phase stability in multi-component systems.^[10–13] These codes can be used to predict the free energy of competing phases as a function of temperature, pressure and composition, and the phases and their

ALI M. NASIRI, Ph.D. Candidate, and DAVID C. WECKMAN and NORMAN Y. ZHOU, Professors, are with the Department of Mechanical & Mechatronics Engineering, Centre for Advanced Materials Joining, University of Waterloo, Waterloo, ON, N2L 3G1, Canada. Contact: e-mail: amnasiri@uwaterloo.ca PATRICE CHARTRAND, Professor, is with the CRCT—Center for Research in Computational Thermochemistry, Department of Chemical Engineering, École Polytechnique, Box 6079, Station Downtown, Montreal, QC H3C 3A7, Canada.

Manuscript submitted July 23, 2012.

Article published online November 9, 2012

compositions that lead to the minimum free energy (i.e., phase equilibrium). The key to all of these computational tools is the database that contains all relevant thermodynamic model parameters required to describe the functional behavior of the Gibbs free energy of all phases, including solutions. The unique feature of these computational thermodynamics tools is that phase equilibrium and thermodynamic properties of multi-component systems corresponding to real commercial alloys with ten or more components can be readily modeled and assessed with reasonable accuracy.

Predicting early stage phase formation along a steel-interlayer-Mg alloy interface can be used to choose the appropriate interlayer between the steel and magnesium alloy. Simulation of the phase formation and thermodynamic properties of the phases during different joining processes, such as laser brazing, can be important tools when developing high temperature joining processes. In this study, computational thermodynamics was used to examine the effect of using a 5- μm -thick Ni interlayer between steel and AZ31B Mg alloy sheet on the phases formed along the steel-fusion zone interface during a laser brazing process using AZ92 Mg brazing alloy.

II. EXPERIMENTAL PROCEDURES

In order to validate the thermodynamic predictions for the steel-Ni-AZ92 system, laser brazing experiments with single-flare bevel lap joints between a 1-mm-thick low alloy plain carbon steel sheet (AISI 1008) with a 5- μm -thick Ni electro-deposited layer and a 2-mm-thick commercial grade twin-roll strip cast AZ31B-H24 magnesium alloy sheet were carried out.^[9] The chemical compositions of the base materials are given in Tables I and II. Figure 1(a) shows the SEM micrograph of a cross section of the nickel-coated steel. The white layer on top of the steel is the Ni coating layer. The coating was of uniform thickness with a void-free interface. EDS analysis of the electro-deposited layer on the steel showed a pure Ni coating layer. A 2.4-mm-diameter TiBrazo Mg 600 filler wire (Mg-Al-Zn alloy) with solidus and liquidus temperatures of 718 K and 873 K (445 °C and 600 °C), respectively, was chosen for this study. The commercial flux used in the experiments was

Table I. Measured Chemical Composition of the AZ31-H24 Mg Alloy Sheet and TiBrazo Mg 600 Filler Metal (Weight Percent)

	Al	Zn	Mn	Si	Mg
AZ31B-H24	3.02	0.80	0.30	0.01	bal.
TiBrazo Mg 600	9.05	1.80	0.18	—	bal.

Table II. Measured Chemical Composition of the 1-mm-Thick Steel Sheet (Weight Percent)

C	Mn	P	S	Fe
0.01	0.5	0.010	0.005	bal.

Superior No. 21 manufactured by Superior Flux and Mfg. Company. This powder flux was composed of LiCl (35 to 40 wt pct), KCl (30 to 35 wt pct), NaF (10 to 25 wt pct), NaCl (8 to 13 wt pct), and ZnCl₂ (6 to 10 wt pct).^[14]

A diagram of the laser brazing apparatus used is shown in Figure 1(b). A Nuvonyx diode laser system with a maximum power of 4.0 kW and a 0.5 × 12 mm laser beam power density distribution was used as a heat source. The beam was focused on top of the filler wire. Laser head manipulation was performed using an integrated Panasonic 6-axis robot. In order to limit oxidation, helium shielding gas was provided in front of the molten pool with a flow rate of 30 L/min from a 6-mm-diameter soft copper feeding tube. The process parameters were laser power, travel speed, and beam position.

After laser brazing, transverse cross sections of the brazed specimens were cut and mounted in epoxy resin. The microstructure and composition of different zones of the joint cross sections were determined using an optical metallurgical microscope and a JEOL JSM-6460

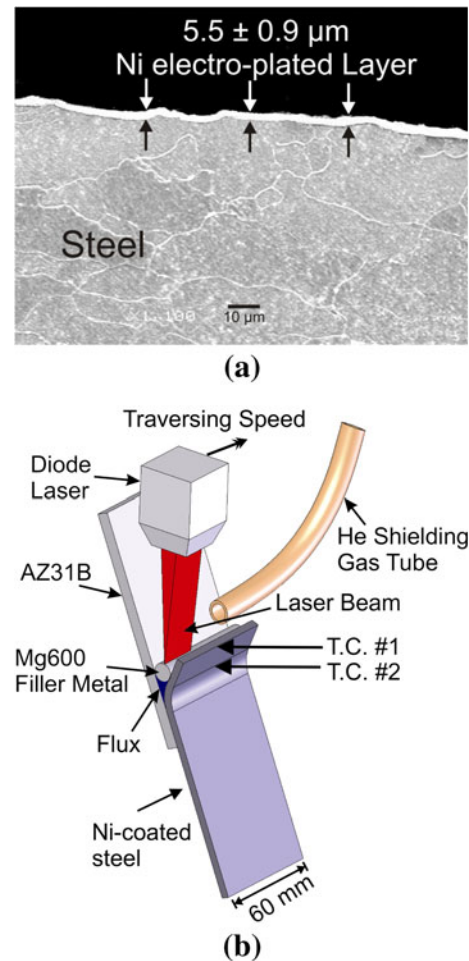


Fig. 1—(a) Transverse section of the Ni electro-deposited layer on the steel substrate and (b) schematic of the laser brazing system used for joining AZ31 Mg and Ni electro-plated steel sheets in the single-flare bevel lap joint configuration showing the position of two thermocouples used for temperature measurements.

scanning electron microscope (JEOL Ltd., Tokyo, Japan) equipped with an Oxford ultrathin window detector energy dispersive X-ray spectrometer (EDS). These experiments and results are described in greater detail in Reference 9.

III. THE THERMOCHEMICAL MODEL

It is well known that welding conditions are far from equilibrium conditions. However, useful estimations can be obtained from thermodynamic models provided that one looks at “local equilibrium.” This assumption is supported by the fact that a liquid state, with high rates of mass transfer, is present in most welding processes. In this study, prediction of early stage phase formation along the steel-Ni-Mg alloy interface was done in two steps. In the first step, with the assumption of full local equilibrium during cooling after the local maximum temperature had been reached, all phases that could possibly form in the steel-Ni-Mg alloy system for a range of temperature and composition were predicted. It was assumed that the time is very short due to a fast heating and cooling rate during the laser brazing process, so mass transfer is constrained to short distances. In the second step, among all the phases that could possibly form, the phase most likely to precipitate first from the liquid at one specific temperature and composition was identified by finding which phase has the highest driving force to form from the liquid phase.

A schematic diagram of the thermochemical model domain that includes the interface between the Ni-plated steel sheet and the AZ92 Mg brazing alloy is shown in Figure 2(a). In order to find the phases that might form in this steel-Ni-Mg alloy system at different temperatures during laser brazing, a ternary system consisting of the steel alloy, Ni interlayer, and Mg alloy (filler metal composition) was defined and its composition field is presented on a Gibbs triangle in Figure 2(b). Since the temperature of the laser brazing process is less than the melting temperature of the steel,^[8] the steel stays in the solid state during this process. Therefore, it was assumed that if the steel participates in any reaction by dissolving into the fusion zone close to the interface, the maximum content of the steel in this system will be low. Thus, the maximum content of the steel alloy in the steel-Ni-Mg alloy system was assumed to be about 10 wt pct as indicated by the dotted tie line in Figure 2(b). In practice, the assumption is that the entire Ni layer can potentially react with the molten AZ92 filler, and the mass of potentially reacting steel components is estimated to be equal to 10 pct of the mass of the Ni layer. The sensitivity of the predicted results to this assumed value was evaluated by performing the same analysis using a lower value of 5 wt pct steel. The results confirmed that in this range, the assumed percentage of steel does not change the predicted results as very similar phase stability maps were generated.

In the laser brazing process, melting of the filler metal by the laser beam occurs initially since the laser is focused on the filler metal. Following this, partial or full dissolution of the Ni interlayer may occur, but very little of the

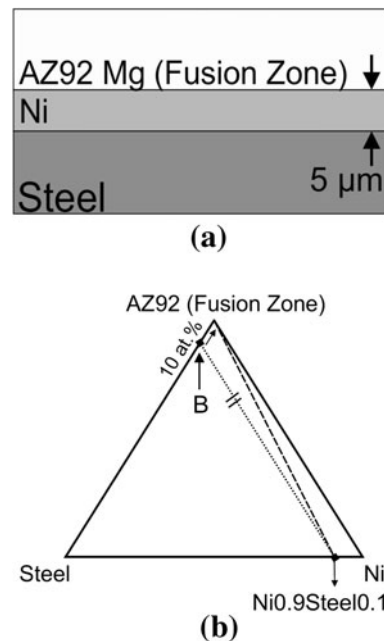


Fig. 2—(a) Schematic of the interface between the Ni-plated steel sheet and the AZ92 Mg brazing alloy and (b) the steel-Ni-Mg alloy ternary system defined in this study.

steel components (Fe-C-Mn) should dissolve as their solubility in Mg-Al-Zn is small. Therefore, immediately after melting of the filler metal and before dissolution of the Ni interlayer into the fusion zone, the steel is not in contact with the fusion zone (see Figure 2(a)). However, point B on the steel-Ni-Mg alloy ternary system (Figure 2(b)) shows that steel and the AZ92 Mg filler metal (FZ) can be in contact with each other. For this reason, point B was moved to the top corner of the ternary system. Therefore, instead of the dotted line in Figure 2(b), the dashed line was considered as a tie line corresponding to a (10 wt pct Steel-Ni)-Mg alloy pseudo-binary system during the laser brazing process.

IV. THERMOCHEMICAL ANALYSIS PROCEDURE

The Phase Diagram module of the commercial thermochemical analysis code FactSage^[10] was used first to generate ternary isothermal sections (in wt pct) in the steel-Ni-Mg alloy system at different temperatures from 873 K to 1373 K (600 °C to 1100 °C). The results are shown in Figures 3(a) through (f). The zero-phase fraction lines for $\text{AlNi}_{(s)}$, $\text{Al}_3\text{Ni}_{5(s)}$, and $\text{Mg}_2\text{Ni}_{(s)}$ are shown. The position of the dashed line in the phase diagrams of Figures 3(a) through (f) shows which phases are predicted to form under local equilibrium conditions during laser brazing at one specific temperature. For example, at 873 K and 973 K (600 °C and 700 °C), Al_3Ni_2 , AlNi , Mg_2Ni , and Al_3Ni_5 are predicted to form. However, from 1073 K to 1373 K (800 °C to 1100 °C), AlNi is the only intermetallic compound that is predicted to form and all other phases are no longer stable.

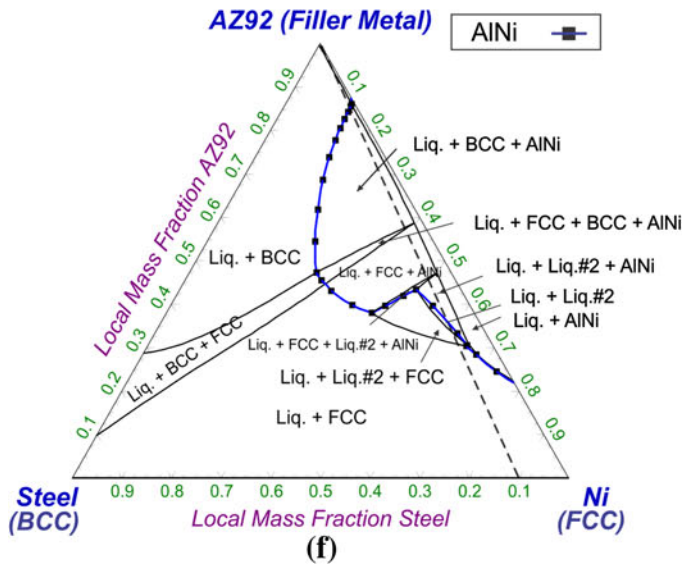
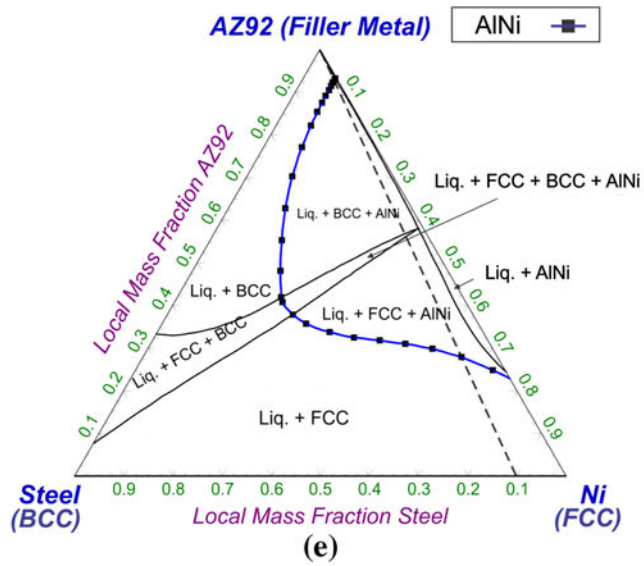
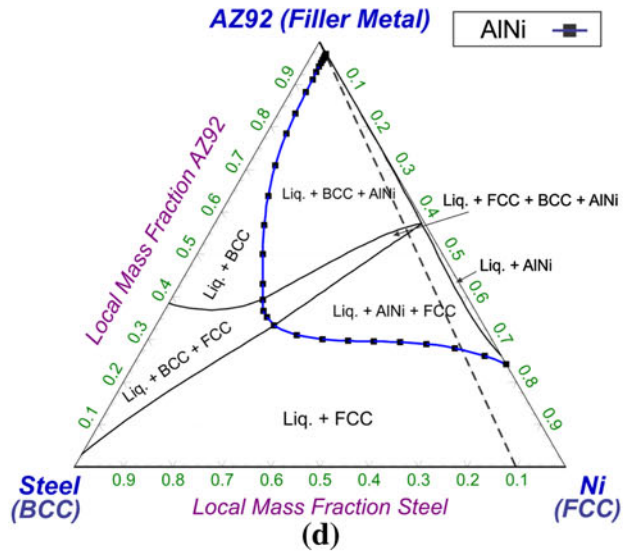


Fig. 3—continued.

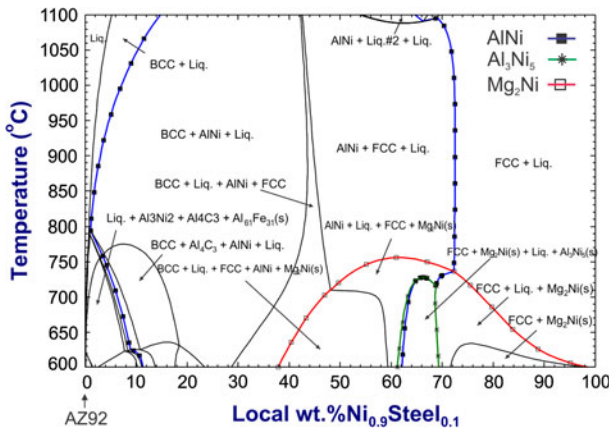
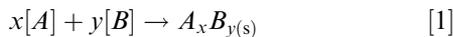


Fig. 4—Predicted AZ92 (filler metal)-Ni_{0.9}Steel_{0.1} binary phase diagram showing the phases that might form along the steel-Ni-Mg alloy interface.

Since each dashed line in Figures 3(a) through (f) is a mass constrain between the AZ92 filler metal and the Ni_{0.9}Steel_{0.1} compositions at a specific temperature, the phases predicted to exist along this line over the temperature range of 873 K to 1373 K (600 °C to 1100 °C) can be used to construct a pseudo-binary system between the AZ92 and the Ni_{0.9}Steel_{0.1} vs temperature as shown in Figure 4. Figure 4 is the calculated isoplethal section (T vs wt pct) along the dashed line in Figures 3(a) through (f). This diagram was used to identify the phases that might form along the steel-Ni-Mg alloy interface at different temperatures during laser brazing. These phases are Al₃Ni, Al₃Ni₂, AlNi, Mg₂Ni, and Al₃Ni₅. All of these phases are binary phases, but may include some minor solubility of a third element. In the next step, the procedure used for finding the first phase most likely to precipitate from the liquid at a specific temperature and composition is explained.

By expressing the composition of a solid phase in the form of a binary compound A_xB_y , the possible reaction for formation of this compound from the liquid in the steel-interlayer (Ni)-Mg alloy system in the laser brazing temperature range can be given as follows:

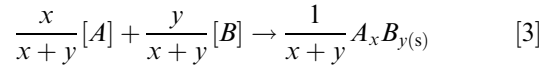


In order to evaluate the stability of the possible precipitated phases, it is important to have a reliable calculation for the change of Gibbs free energy, ΔG , of the reaction shown in Eq. [1]. A negative ΔG indicates that the reaction will proceed spontaneously to the right, whereas a positive ΔG indicates that the reaction shown in Eq. [1] will proceed spontaneously from right to left.

The standard Gibbs free energy change with the formation of a solid phase from the pure liquid components (given as $[A]$ and $[B]$) (ΔG°) indicated in Eq. [1] can be determined using^[15]

$$\Delta G_{T,(A_xB_y)}^\circ = -RT \ln \frac{a(A_xB_y)}{a^x([A])a^y([B])} \quad [2]$$

where R is the Universal Gas constant, T is the absolute temperature (K), and a is the chemical activity of each phase. For 1 mol of the elements, we have



and, therefore,

$$\Delta G_{T,(A_{x/x+y}B_{y/x+y})}^\circ = -RT \ln \left(\frac{a(A_xB_y)}{a^x([A])a^y([B])} \right)^{\frac{1}{x+y}} \quad [4]$$

After local fusion of the “system,” for a given local temperature and local composition, which fixes the chemical activity of $[A]$ and $[B]$ in the liquid state, the chemical activity of $A_xB_{y(s)}$ can be computed when $\Delta G_{(T)}^\circ$ is known (from the databases). At equilibrium, if $[a(A_xB_y)]^{1/x+y} > 1$, then A_xB_y should form spontaneously. The stability and driving force for formation of the phase increase with increasing activity. Therefore, the first precipitated phase from the liquid at a specific temperature and composition will be the phase with the maximum activity value, but only if this activity is greater than unity. This concept can be used when there are many possible phases predicated and we are not really sure which, if any, will form. Considering the phases that might form along the steel-Ni-Mg alloy interface, for 1 mol of the system, the following reactions and net change in free energy are possible:

0.75 mol Al + 0.25 mol Ni will form 0.25 mol of Al₃Ni

with a change of Gibbs free energy of

$$\Delta G_{T,(Al_{3/4}Ni_{1/4})}^\circ = -RT \ln \left(\frac{a(Al_3Ni)}{a^3([Al])a([Ni])} \right)^{\frac{1}{4}} \quad [5]$$

Similarly,

0.60 mol Al + 0.40 mol Ni will form 0.20 mol of Al₃Ni₂

with a change of Gibbs free energy of

$$\Delta G_{T,(Al_{3/5}Ni_{2/5})}^\circ = -RT \ln \left(\frac{a(Al_3Ni_2)}{a^3([Al])a^2([Ni])} \right)^{\frac{1}{5}} \quad [6]$$

0.50 mol Al + 0.50 mol Ni will form 0.50 mol of AlNi

with a change of Gibbs free energy of

$$\Delta G_{T,(Al_{1/2}Ni_{1/2})}^\circ = -RT \ln \left(\frac{a(AlNi)}{a([Al])a([Ni])} \right)^{\frac{1}{2}} \quad [7]$$

0.375 mol Al + 0.625 mol Ni will form 0.125 mol of Al₃Ni₅

with a change of Gibbs free energy of

$$\Delta G_{T,(Al_{3/8}Ni_{5/8})}^\circ = -RT \ln \left(\frac{a(Al_3Ni_5)}{a^3([Al])a^5([Ni])} \right)^{\frac{1}{8}} \quad [8]$$

and

0.666 mol Mg + 0.333 mol Ni will form 0.333 mol of Mg₂Ni with a change of free energy of

$$\Delta G_{T,(\text{Mg}_{2/3}\text{Ni}_{1/3})}^{\circ} = -RT \ln \left(\frac{a(\text{Mg}_2\text{Ni})}{a^2([\text{Mg}])a([\text{Ni}])} \right)^{\frac{1}{3}} \quad [9]$$

The component activities were evaluated using the Equilib module of FactSage^[10] at different laser brazing temperatures. The activity-composition diagrams for Al₃Ni, Al₃Ni₂, AlNi, Mg₂Ni, and Al₃Ni₅ from 873 K to 1373 K (600 °C to 1100 °C) are shown in Figure 5. At 873 K and 973 K (600 °C to 700 °C), Al₃Ni₂, AlNi, and Mg₂Ni are predicted to be the first precipitated phases from the liquid at different composition ranges (mass fraction of Ni_{0.9}Steel_{0.1}). Note that the composition here should be seen as an approximated position between the filler ($x = 0$) and an initial position within the steel just next to the Ni-steel interface ($x = 1$), where the mass ratio of Ni to steel is roughly 10 to 1. In the temperature range of 1073 K to 1373 K (800 °C to 1100 °C), AlNi is predicted to be the first and only precipitated phase from the liquid. Using this calculation procedure, a phase stability map, shown in Figure 6, was plotted indicating the first precipitated phases from the liquid at different temperatures and compositions during the laser brazing process. This stability map suggests that at temperatures higher than 873 K (600 °C), immediately adjacent to the Ni_{0.9}Steel_{0.1} (*i.e.*, when $x \rightarrow 1$, on the steel side), there will likely be a layer of liquid very rich in Ni_{0.9}Steel_{0.1} at most temperatures. When the temperature of this liquid drops below about 998 K (725 °C), Mg₂Ni will likely form between the Ni_{0.9}Steel_{0.1} and the AlNi. When the Ni_{0.9}Steel_{0.1} composition of the AZ92 liquid drops below about 0.72 mass fraction, AlNi will likely form over a large composition range (0.02 to 0.72 mass fraction of Ni_{0.9}Steel_{0.1}). At temperatures higher than 1048 K (775 °C), when the mass fraction of Ni_{0.9}Steel_{0.1} in the liquid drops below 0.02 to 0.15 further away from the interface, the liquid will be mostly AZ92. When the temperature drops below about 1048 K (775 °C), there may be a thin band of Al₃Ni₂ formed between the AlNi and the AZ92 filler metal. Note that on Figures 5(a) and (b), the chemical activity of Al₃Ni₂ is barely greater than the one of AlNi, suggesting a very small difference of driving forces for forming these phases from the liquid solution.

V. COMPARISON WITH EXPERIMENTAL RESULTS

In order to validate the thermodynamic predictions for the steel-Ni-AZ92 system, laser brazing experiments with single-flare bevel lap joints between a plain low carbon steel sheet with a 5- μm -thick Ni electro-deposited layer and AZ31B-H24 magnesium alloy sheet were performed.^[9] Figure 7 shows the microstructure at different locations at the steel-FZ interface. A detailed

description of the microstructures in the fusion zone and the AZ31B Mg-H24 alloy sheet may be found in Reference 8. The Ni coating was not detected as a separate layer along the interface after laser brazing. This suggests that it had entirely melted and gone into the solution in the liquid immediately adjacent to the interface. It was observed that the microstructure of the FZ-steel interface changed significantly across the FZ-steel interface from the bottom (position A, Figure 7(b)) to the top (position C, Figure 7(d)) side of the joint. In order to help explain this change of microstructure during the laser brazing process, the temperature distribution across the interface vs time was measured during laser brazing using two thermocouples, one attached to the top side and the other to the bottom side of the steel sheet (see Figure 1(b)). According to the measured temperature profiles shown in Figure 8, the steel sheet experienced maximum temperatures of 1424 K and 926 K (1151 °C and 653 °C) on the top and the bottom side, respectively. Therefore, a 773 K (500 °C) temperature gradient was measured between the top and the bottom side of the steel sheet during the laser brazing process. This was because the laser beam was focused on the top of the filler wire as shown in Figure 1(b).^[9] This temperature difference and gradient across the joint interface during the laser brazing process is believed to be the main reason for the prominent change of microstructure across the FZ-steel interface.

As shown in Figure 7(b), at the bottom of the interface at A, a few diamond-shaped bright phases were formed near the steel-FZ interface. According to an EDS analysis of the diamond-shaped bright phases shown in Figure 7(b), the composition of the particles was 49.6 ± 1.3 at. pct Ni, 45.4 ± 4.7 at. pct Al, and 5.0 ± 2.5 at. pct Mg, thus confirming that the diamond-shaped particles were mainly composed of AlNi intermetallic compound (IMC). These results were confirmed by XRD and also Selected Area Diffraction Pattern (SADP) analysis and STEM EDS results.^[9] Closer to the interface, the AlNi has grown with a faceted dendritic morphology. Also at A, some gray lamellar phases, as shown in Figure 7(b), were observed between the AlNi IMC layer and the steel. According to our previous study,^[9] this region contained lamellar phases including white lamellae corresponding to “ α -Mg eutectic” and dark lamellae containing 27.6 ± 7.2 at. pct Ni and 72.3 ± 7.3 at. pct Mg representing the Mg₂Ni stoichiometric intermetallic compound confirmed by the SADP analysis. These two phases next to each other are the α -Mg-Mg₂Ni lamellar eutectic.^[9] Finally, the darkest round phase between the eutectic and the AlNi dendrites consists of particles of the primary α -Mg phase.^[9]

It was observed that upon moving from the bottom to the middle of the interface (region B in Figure 7(a)), which was associated with increasing temperature, the morphology of the IMC phase along the interface changed from the diamond-shaped AlNi to a faceted dendritic-shaped phase (see Figure 7(c)). EDS analysis results indicated this dendritic phase contained 43.0 ± 1.6 at. pct Ni, 52.1 ± 2.0 at. pct Al, and 4.9 ± 0.5 at. pct Mg. This composition again corresponded with the AlNi IMC phase.^[9] In this area, the

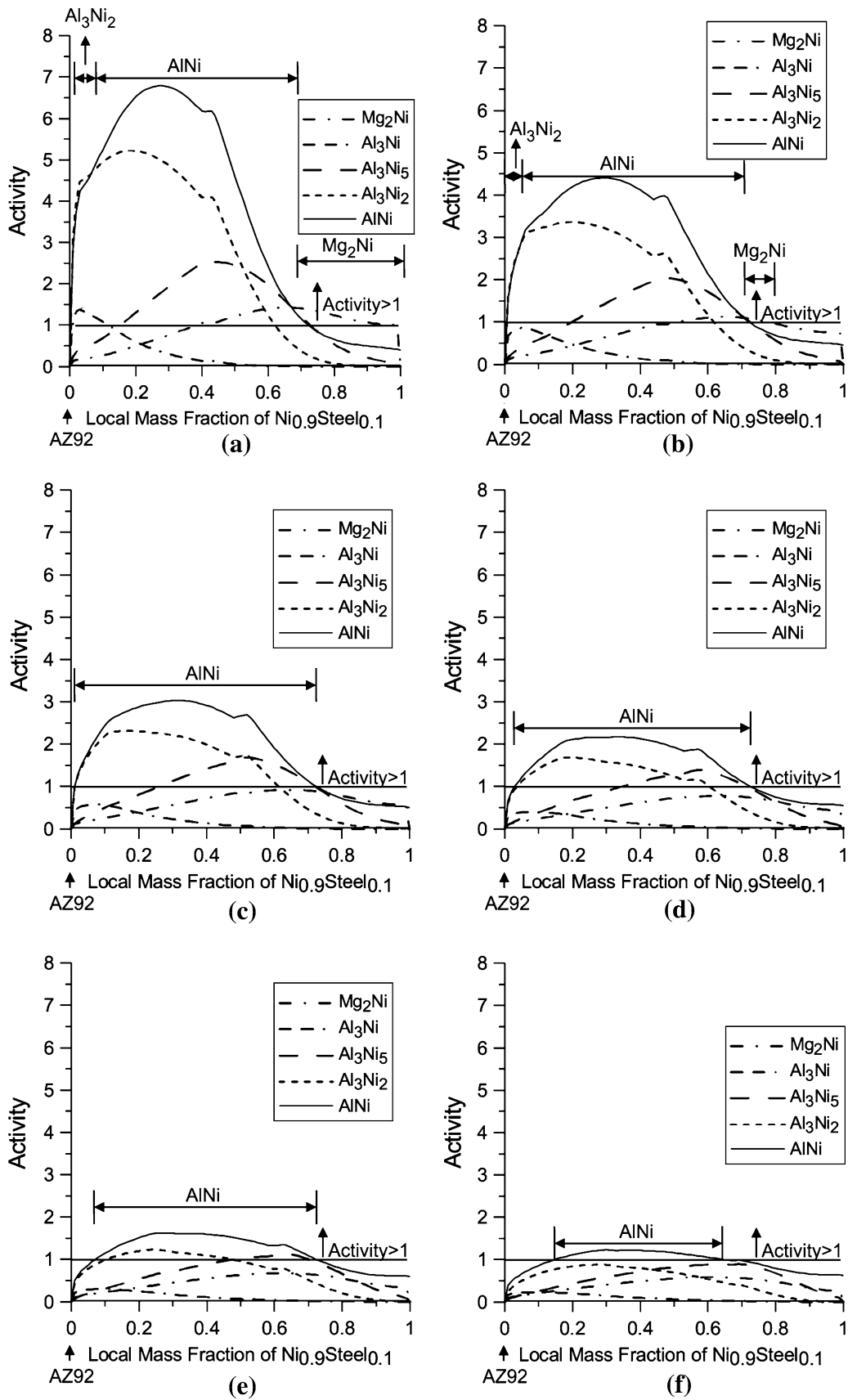


Fig. 5—The activity-composition diagrams for AlNi, Al₃Ni₂, Al₃Ni₅, Al₃Ni, and Mg₂Ni at (a) 873 K (600 °C), (b) 973 K (700 °C), (c) 1073 K (800 °C), (d) 1173 K (900 °C), (e) 1273 K (1000 °C), and (f) 1373 K (1100 °C).

first precipitated phase from the liquid was AlNi IMC, the same as at the bottom of the joint. This phase grew steadily in a faceted dendritic shape. As the interface temperature increased with moving from position A to position B in Figure 7(a), the growth morphology of AlNi changed from diamond shaped to a dendritic shape, as demonstrated in Figure 7(c). Continuous growth of the AlNi was observed in this area with some dendrites having long secondary dendrite arms (see Figure 7(c)).

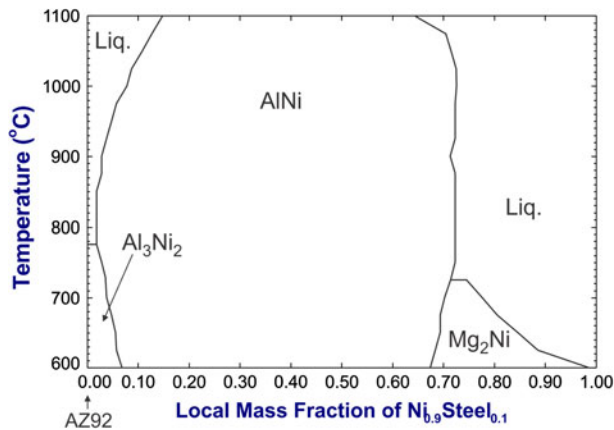


Fig. 6—Phase stability map showing the first precipitated phases from the liquid at different temperatures and compositions during the laser brazing process.

At the top side of the joint (position C in Figure 7(a)), the morphology of the interfacial phase changed further and a high volume fraction of a nodular phase with the composition of 48.4 ± 1.4 at. pct Ni, 50.1 ± 1.2 at. pct Al, and 1.5 ± 0.4 at. pct Mg was detected (Figure 7(d)). This phase was also found to be the AlNi IMC phase.^[9] Detailed microstructural analysis of the fusion zone-steel

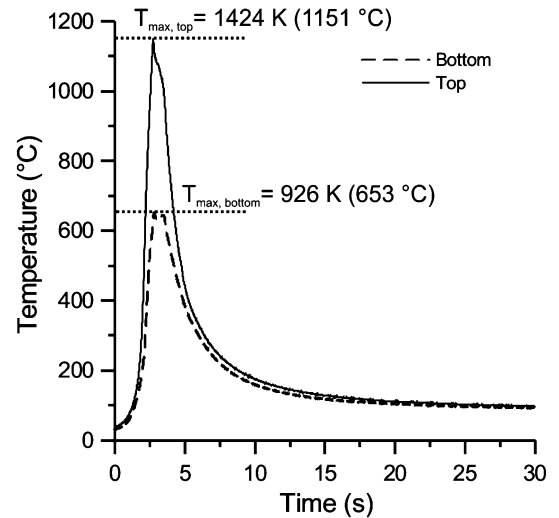


Fig. 8—Typical temperature vs. time profiles measured during laser brazing at the top and bottom side of the joint.

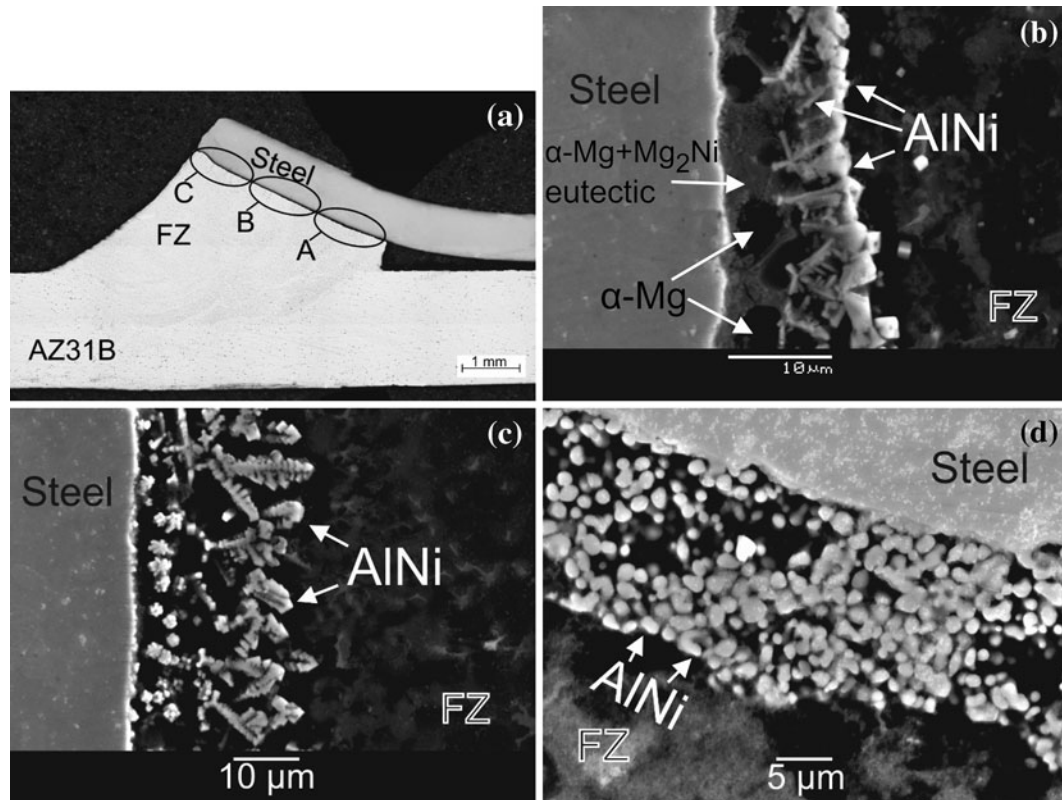


Fig. 7—SEM images of the laser-brazed specimen in different positions of the steel-FZ interface shown in (a): (b) position A, (c) position B, and (d) position C.

interface after the laser brazing process has been reported in our previous investigation.^[9]

These experimental results have confirmed the formation of dendritic AlNi IMC and also α -Mg + Mg₂Ni phases along the interface at the bottom of the joint (Figure 7(b)), where measured temperatures during the process were close to 973 K (700 °C), and just a dendritic AlNi phase along the interface at the middle and top side of the joint (Figures 7(c) and (d)), where the measured temperatures were more than 1073 K (800 °C). These experimental results are in agreement with the predicted phase stability map shown in Figure 6 at 973 K (700 °C) and more than 1073 K (800 °C).

The Al₃Ni₂ IMC that was predicted to form by the thermochemical analysis was not detected along the steel/FZ interface after the laser brazing process. According to the Al-Ni binary phase diagram, Al₃Ni₂ forms after formation of AlNi as a result of a peritectic reaction. Since this reaction proceeds much more slowly than monotectic reactions (formation of AlNi) or eutectic reactions (formation of α -Mg + Mg₂Ni),^[16] the very fast cooling rates experienced during the laser brazing process must prevent the formation of this phase. Therefore, some additional features must be taken into account when attempting to predict phase formation in a complex system based on such thermochemical calculations. While useful estimations and predictions can be obtained from thermodynamic models based on the assumption of local equilibrium, when dealing with welding and brazing processes, the high cooling rates and solute microsegregation that take place during solidification can lead to many non-equilibrium effects. For instance, some phases that are not stable in the equilibrium condition may become stable as a result of solute enrichment during solidification. Second, the calculations do not consider phase transformation kinetics. When trying to predict the microstructure or possible formed phases, the kinetic considerations should be taken into account. Some kinetic calculations based on diffusion-controlled mechanisms tied in with the computational thermodynamic approach are possible with available software.^[17]

VI. CONCLUSIONS

In the present work, a computational thermodynamic analysis using FactSage thermochemical software was performed to predict the phases most likely to form along the interface between Ni electro-plated steel and AZ92 Mg alloy (filler metal composition) sheets during

the laser brazing process. Calculations were done over a wide temperature and composition range. It was concluded that the addition of the Ni interlayer between the steel and the AZ92 Mg alloy may lead to the formation of the AlNi, Mg₂Ni, and Al₃Ni₂ intermetallic compounds along the steel/fusion zone interface, where the AlNi and Mg₂Ni are most likely to form under non-equilibrium conditions present during laser brazing. Experimental results have confirmed these predictions.

ACKNOWLEDGMENTS

The authors wish to acknowledge support from the American Welding Society (AWS) Graduate Fellowship program, the Natural Sciences and Engineering Research Council of Canada (NSERC), and the Magnesium Network of Canada (MagNET) for sponsoring this work.

REFERENCES

1. J. Yan, Z. Xu, Z. Li, L. Li, and S. Yang: *Scripta Mater.*, 2005, vol. 53, pp. 585–89.
2. L. Liu: *Welding and Joining of Magnesium Alloys*, Woodhead Publishing Ltd., Cambridge, 2010.
3. L. Liu, L. Xiao, J. Feng, L. Li, S. Esmaili, and Y. Zhou: *Scripta Mater.*, 2011, vol. 65, pp. 982–85.
4. X. Zhao, G. Song, and L. Liu: *Trans. Chin. Weld. Inst.*, 2006, vol. 27, pp. 56–62.
5. X. Qi and G. Song: *Mater. Des.*, 2010, vol. 31, pp. 605–09.
6. L. Liu, X. Qi, and Z. Wu: *Mater. Lett.*, 2010, vol. 64, pp. 89–92.
7. L.M. Liu and X. Qi: *J. Mater. Sci.*, 2009, vol. 44, pp. 5725–31.
8. A.M. Nasiri, L. Li, S.H. Kim, Y. Zhou, D.C. Weckman, and T.C. Nguyen: *Weld. J.*, 2011, vol. 90 (11), pp. 211–19.
9. A.M. Nasiri, D.C. Weckman, and Y. Zhou: *Weld. J.*, 2013, vol. 92 (1), p. 1.
10. C.W. Bale, E. Bêlisle, P. Chartrand, S.A. Deckerov, G. Eriksson, K. Hack, I.H. Jung, Y.B. Kang, J. Melançon, A.D. Pelton, C. Robelin, and S. Petersen: *CALPHAD*, 2009, vol. 33, pp. 295–311.
11. N. Saunders, X. Li, A.P. Miodownik, and J.P. Schille: in *Computer Modelling of Materials Properties*, J.C. Zhao, M. Fahrman, and T. Pollock, eds., TMS, Warrendale, PA, 2001, pp. 185–97.
12. R.H. Davies, A.T. Dinsdale, J.A. Gisby, J.A.J. Robinson, and S.M. Martin: *CALPHAD*, 2002, vol. 26, pp. 229–71.
13. S.L. Chen, S. Daniel, F. Zhang, Y.A. Chang, X.Y. Yan, F.Y. Xie, R. Schmid Fetzer, and W.A. Oates: *CALPHAD*, 2002, vol. 26, pp. 175–88.
14. Material Safety Data Sheet: Superior Flux & Mfg. Co., 2003, p. 1.
15. D.R. Gaskell: *Introduction to Metallurgical Thermodynamics*, 2nd ed., Hemisphere Publishing Corp., New York, 1981.
16. M.C. Flemings: *Solidification Processing*, McGraw-Hill, New York, 1974, pp. 157–60.
17. J.O. Andersson, T. Helander, L. Hogland, P. Shi, and B. Sundman: *CALPHAD*, 2002, vol. 26, pp. 273–312.